NORMALIZED DISTRIBUTIONS OF NANODIAMOND $^{12}C/^{13}C$ ISOTOPIC RATIOS FROM ALLENDE BY ATOM-PROBE TOMOGRAPHY. J. B. Lewis[1], D. Isheim[2], C. Floss[1], D. N. Seidman[2], [1]Laboratory for Space Sciences, Physics Dept., Washington University, St. Louis, MO. [2]Center for Atom-Probe Tomography, Dept. of Materials Science and Engineering, Northwestern University, Evanston, IL. Email: jblewis@go.wustl.edu

Introduction: Discovered in 1987 and present in chondrites in levels up to 14,000 ppm, meteoritic nanodiamonds may originate from outside the solar system, as evidenced by the presence of the *s*- and *r*-process component Xe-HL [1–3]. However, C and N isotopic compositions suggest a solar origin [4,5]. The distribution of isotopic ratios in individual meteoritic nanodiamonds is key to determining whether they originated in the solar system or from a presolar source such as supernovae or the interstellar medium. The average nanodiamond contains only ~2000 atoms [6], too few for direct isotopic assessment by traditional methods [4]. Efforts are ongoing to adapt atom-probe tomography (APT) to measure the $^{12}C/^{13}C$ isotopes of individual nanodiamonds [7–9]. We discuss the implications of $^{12}C/^{13}C$ isotopic ratios calculated from 30 APT data sets containing on the order of 100 individual meteoritic nanodiamonds in total.

Methods: We deposited nanodiamond acid residue from the carbonaceous chondrite Allende (CV3) [1] onto an ion-beam-sputter-deposited Pt layer, deposited additional Pt to embed the nanodiamonds in a Pt-sandwich, and conducted cross-sectional focused ion beam liftout and milling to shape the samples into the ultrasharp (less than 100 nm radius) nanotips required for APT analysis [8]. For isotopic normalization we used the same methodology to prepare nanotips containing synthetic detonation nanodiamonds [10].

We analyzed the nanotips using the LEAP 4000X Si atom-probe tomograph at Northwestern University. This instrument field-evaporates individual atoms from the nanotip as ions using a standing high voltage and thermal pulses from a UV laser. The electric field lines created by the standing voltage accelerate the ions onto a detector (50% detection efficiency) with a point-projection geometry. The time of flight of each ion from laser pulse to detection and the order in which the ions are detected is used to reconstruct each data set into a 3D representation of the original nanotip along with mass-to-charge-state data for each detected ion. Reconstructions have sub-nm spatial resolution and sufficient mass resolution to easily distinguish ^{12}C and ^{13}C ions in charge states one and two: C^{+} and C^{++}. We correct the C counts for background, overlapping tails from nearby peaks, and signal loss from detector multi-hits. Over several years we have collected enough data from Allende nanodiamonds for statistical analysis, and enough detonation nanodiamond data to assess instrumental artifacts and normalize the Allende data sets [7–9,11].

We calculated the weighted mean $^{12}C^{+}/^{13}C^{+}$ and $^{12}C^{++}/^{13}C^{++}$ for 26 detonation nanodiamond data sets: 73(+101,-27) for C^{+}, 52(+24,-13) for C^{++}, and normalized the ratios in each meteoritic data set to these estimations of the terrestrial value. Ten of the detonation nanodiamond sets were previously unpublished. Uncertainties in the $^{12}C/^{13}C$ ratios are asymmetric because the denominator ^{13}C often has low counts, making the ratio asymmetrically affected by the positive and negative uncertainty from counting statistics.

Data: We reduced twelve new APT data sets from Allende nanodiamonds and calculated the $^{12}C/^{13}C$ isotopic ratios of the nanodiamond acid residue. These are plotted in Figure 1, along with 18 previously published Allende nanodiamond data sets, all normalized to the detonation nanodiamonds, such that data points lying along the terrestrial line are in agreement with the mean detonation nanodiamond ratios reported in the methods section. The mean $\delta^{13}C^{+}$ isotopic anomaly is (-18±24)‰ with a large standard deviation of 620‰, and the mean $\delta^{13}C^{++}$ isotopic anomaly is (-192±24)‰ with a standard deviation of 410‰.

Discussion: Our data show that the assortment of nanodiamonds we have measured have $^{12}C/^{13}C$ ratios that, on average, are in agreement with studies of billions of nanodiamonds by stepped combustion, which established the ratio of $^{12}C/^{13}C$ to lie in the range $\delta^{13}C$ = 20–40‰ [4,12]. These mean values are consistent with a solar system formation of the nanodiamonds and do not provide evidence of a presolar origin.

The acid residues in each nanotip contain on the order of 10 individual nanodiamonds, but some of the carbonaceous material in the residues may be sp2-bonded amorphous C [13]. Therefore, it is possible that individual nanotips contain nanodiamonds and sp2-bonded C from multiple sources, which have different $^{12}C/^{13}C$ isotopic ratios that are averaging to the values presented here.

Three of the data sets stand out as being significantly enriched in ^{13}C. However, they have large uncertainties: Compared to the solar system $^{12}C/^{13}C$ ratio of 90 [14], R06 19354 has $^{12}C^{+}/^{13}C^{+}$ = 17(+39,-7) and $^{12}C^{++}/^{13}C^{++}$ = 59(+1185,-29). R06 23612 and 23617 have $^{12}C^{+}/^{13}C^{+}$ ratios of 38(+87,-15) and 26(+54,-11), respectively (there were not enough counts to calculate $^{12}C^{++}/^{13}C^{++}$ ratios). The large error bars are the result of both low counts and the large scatter in the measured ratios of the terrestrial nanodiamonds. If the scatter of the standards is not assessed as an uncertainty, we would use σ/n, the standard error of the mean, as the uncertainty in the mean value of the detonation data sets, rather than σ, greatly reducing the uncertainties.

If these data points do represent the isotopic composition of the nanodiamonds in those nanotips, they could be produced by supernovae, which can create a wide range of C isotopic anomalies, and can also produce the Xe-HL anomaly observed in the nanodiamonds in other studies.

References: [1] Lewis R. S. et al. (1987) *Nature, 326*, 160–162. [2] Lewis R. S. et al. (1989) *Nature, 339*, 117–121. [3] Zinner E. (2014) Presolar Grains *Treatise on Geochemistry* vol 1(Elsevier) pp. 181–213. [4] Russell S. S. et al. (1996) *Meteoritics & Planet. Sci., 31*, 343–355. [5] Marty B. et al. (2011) *Science, 332*, 1533–1536. [6] Daulton T. L. et al. (1996 *Geochim. Cosmochim. Acta, 60*, 4853–4872. [7] Heck P. R. et al. (2014) *Meteoritics & Planet. Sci., 49*, 453–467. [8] Isheim D. (2013) *Microsc. Microanal., 19*, 974–975. [9] Lewis J. B. et al. (2015) *Ultramicroscopy, 159, Part 2*, 248–254. [10] Greiner N. R. et al. (1988) *Nature, 333*, 440–442. [11] Lewis, J. B. et al. (2015) *LPS XLVI*, Abstract #1480. [12] Swart P. K. et al. (1983) *Science, 220*, 406–410. [13] Stroud R. M. et al. *Astrophys. J., 738*, L27. [14] Coplen T. B. et al. (2002) *Pure Appl. Chem., 74*, 1987–2017.

This work is supported by NASA grants NNX14AP15H (J.B.L.) and NNX16AD26G (C.F.). The LEAP tomograph at NUCAPT was acquired and upgraded with NSF DMR-0420532 and ONR-DURIP N00014-0400798, N00014-0610539, N00014-0910781 equipment grants. NUCAPT received support from the MRSEC program (NSF DMR-1121262) at the Materials Research Center, the SHyNE Resource (NSF NNCI-1542205), and the Initiative for Sustainability and Energy at Northwestern (ISEN)).

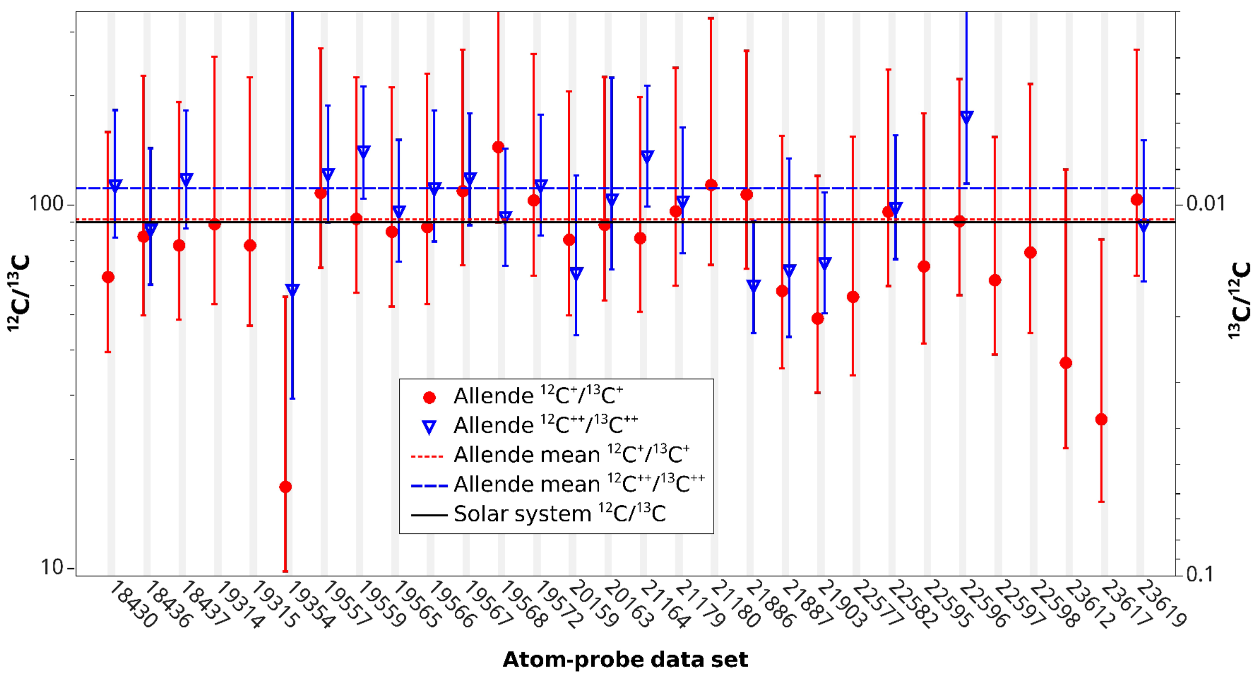

Figure 1: $^{13}C/^{12}C$ isotopic ratios for 30 atom-probe data sets. The ratios are normalized using the mean $^{13}C/^{12}C$ from 26 data sets of terrestrial synthetic detonation nanodiamond standards. The solar system value, $^{12}C/^{13}C$=90, is denoted by the black line. The small-dashed red line and large-dashed blue line denote the mean $^{12}C^{+}/^{13}C^{+}$ and $^{12}C^{++}/^{13}C^{++}$ ratios, respectively. Data set ID numbers are presented along the x-axis, all collected at Northwestern University. The plot is logarithmic in $^{13}C/^{12}C$ ratio, denoted on the right-hand side. On the left-hand side, the $^{12}C/^{13}C$ ratio is given for ease of reading. Error bars are 1σ and include the uncertainty due to normalization, as well as counting statistics, background, and detector multihit corrections. Data sets R06 18430–18437 were previously published in [7], and data sets R06 19314–21180 were previously published in [9].